

Pantoprazole, a Proton Pump Inhibitor, Delays Fracture Healing in Mice

T. Histing · D. Stenger · C. Scheuer ·
W. Metzger · P. Garcia · J. H. Holstein ·
M. Klein · T. Pohlemann · M. D. Menger

Received: 4 November 2011 / Accepted: 1 April 2012 / Published online: 24 April 2012
© Springer Science+Business Media, LLC 2012

Abstract Proton pump inhibitors (PPIs), which are widely used in the treatment of dyspeptic problems, have been shown to reduce osteoclast activity. There is no information, however, on whether PPIs affect fracture healing. We therefore studied the effect of the PPI pantoprazole on callus formation and biomechanics during fracture repair. Bone healing was analyzed in a murine fracture model using radiological, biomechanical, histomorphometric, and protein biochemical analyses at 2 and 5 weeks after fracture. Twenty-one mice received 100 mg/kg body weight pantoprazole i.p. daily. Controls ($n = 21$) received equivalent amounts of vehicle. In pantoprazole-treated animals biomechanical analysis revealed a significantly reduced bending stiffness at 5 weeks after fracture compared to controls. This was associated with a significantly lower amount of bony tissue within the callus and higher amounts of cartilaginous and fibrous tissue. Western blot analysis showed reduced expression of the bone formation markers bone morphogenetic protein (BMP)-2,

BMP-4, and cysteine-rich protein (CYR61). In addition, significantly lower expression of proliferating cell nuclear antigen indicated reduced cell proliferation after pantoprazole treatment. Of interest, the reduced expression of bone formation markers was associated with a significantly diminished expression of RANKL, indicating osteoclast inhibition. Pantoprazole delays fracture healing by affecting both bone formation and bone remodeling.

Keywords Fracture repair · Bone healing · RANKL · Bone formation marker · Bone remodeling

Acid-suppression medications such as proton pump-inhibitors (PPIs) are among the most widely prescribed medications worldwide. PPIs are commonly used drugs for the therapy of reflux esophagitis, peptic ulcers, and other acid-related gastrointestinal disorders [1]. In addition, PPIs are used in combination with an analgetic therapy, first of all with nonsteroidal anti-inflammatory drugs (NSAIDs), to avoid stress ulcers by inhibition of gastric proton-pump ($H^+/K^+-ATPase$) activity in the final step of gastric acid secretion in parietal cells [2]. Recent studies have reported potential adverse consequences of chronic acid suppression, including an increased risk for bone fractures. Stomach acid and the slightly acidic milieu of the proximal duodenum are necessary for calcium absorption. Consequently, PPI therapy may cause a negative calcium balance, resulting in an increased rate of bone loss and a greater risk of fracture [3, 4]. Targownik et al. [5] reported also that the use of PPIs is associated with an increased risk of osteoporosis-related fractures. Other studies showed that PPI therapy, particularly at high doses, is associated with an increased risk of hip [6] and nonspine [7] fractures. Finally, long-term use of PPIs decreases vitamin B₁₂

The first two authors contributed equally to this work.

T. Histing (✉) · D. Stenger · W. Metzger · P. Garcia ·
J. H. Holstein · M. Klein · T. Pohlemann
Department of Trauma, Hand, and Reconstructive Surgery,
University of Saarland, 66421 Homburg/Saar, Germany
e-mail: tina.histing@uks.eu

T. Histing · D. Stenger · C. Scheuer · W. Metzger · P. Garcia ·
J. H. Holstein · M. Klein · T. Pohlemann · M. D. Menger
CRC Homburg (Collaborative Research Center),
AO Foundation, Davos, Switzerland

C. Scheuer · M. D. Menger
Institute for Clinical & Experimental Surgery, University of
Saarland, 66421 Homburg/Saar, Germany

resorption, which may also be associated with low bone mineral density (BMD) and fractures [8].

On the other hand, *in vitro* and human data suggest that PPIs decrease bone resorption by inhibiting osteoclastic vacuolar H⁺-ATPase [9–11]. Vacuolar H⁺-ATPases are present in high concentration on the ruffled border of the resorbing osteoclasts, and this proton pump extrudes protons during the bone resorption process. Of interest, administration of a selective inhibitor of the osteoclastic vacuolar H⁺-ATPase prevents bone loss in ovariectomized rats. These findings raise the possibility that PPIs can prevent osteoporosis and fractures [12].

While there are these controversial data on whether PPIs induce or prevent bone loss, there is a complete lack of information on whether PPIs influence the process of bone healing and regeneration. Therefore, we studied the effects of pantoprazole on fracture healing in a standardized femur fracture model in mice.

Materials and Methods

Animals and Specimens

CD-1 mice were bred at the Institute for Clinical and Experimental Surgery, University of Saarland. They were kept on a 12-hour light and dark cycle and fed a standard diet with water *ad libitum*. All animal procedures were performed according to the National Institutes of Health guidelines for the use of experimental animals and the German legislation on the protection of animals. For the present study a total of 42 animals, 12–14 weeks old, were used. Twenty-one mice were treated daily *i.p.* with 100 mg/kg body weight (BW) pantoprazole (Nycomed, Konstanz, Germany). Another 21 vehicle (saline)-treated mice served as controls. We are aware that the dose of 100 mg/kg pantoprazole per day is substantially higher than the doses given in daily clinical practice in humans. However, in experimental studies, in particular in proof-of-principle studies, doses of pantoprazole ranging between 1 and 300 mg/kg/day are reported in mice and rats [13, 14]. Accordingly, we chose a dose of 100 mg/kg/day in the present study.

Surgical Procedure

Mice were anesthetized by *i.p.* injection of xylazine (25 mg/kg BW) and ketamine (75 mg/kg BW). A 4-mm medial parapatellar incision was performed at the right knee to dislocate the patella laterally. After drilling a hole (0.5 mm in diameter) into the intracondylar notch, an injection needle with a diameter of 0.4 mm was drilled into the intramedullary canal. Subsequently, a tungsten

guidewire (0.2 mm in diameter) was inserted through the needle into the intramedullary canal. After removal of the needle, the femur was fractured by a three-point bending device and an intramedullary titanium screw (18 mm length, 0.5 mm in diameter; AO Foundation, Research Implants Systems, Davos, Switzerland) was implanted over the guidewire to stabilize the fracture [15]. Fracture and implant position were confirmed by radiography.

Radiological Analysis

At the end of the 2- and 5-week observation periods the animals were reanesthetized and ventrodorsal radiographs of the healing femora were performed. Fracture healing was analyzed according to the classification of Goldberg, with stage 0 indicating radiological non-union, stage 1 indicating possible union, and stage 2 indicating radiological union [16].

Biomechanical Analysis

For biomechanical analysis, the right and left femora were resected at 2 ($n = 8$ each group) and 5 ($n = 8$ each group) weeks and freed from soft tissue. After removing the implants, callus stiffness was measured with a nondestructive test using a three-point bending device (Mini-Zwick Z 2.5; Zwick, Ulm, Germany). Due to the different stages of healing, the loads which had to be applied varied markedly between the individual animals. Loading was stopped individually in every case when the actual load–displacement curve deviated more than 1% from linearity. To account for differences in bone stiffness of the individual animals, the unfractured left femora were also analyzed, serving as an internal control. All values of the fractured femora are given as absolute values and in percent of the corresponding unfractured femora. Bending stiffness (N/mm) was calculated from the linear elastic part of the load–displacement diagram [17].

Histomorphometric Analysis

For histology, eight bones of each group were analyzed at 2 and 5 weeks after fracture healing. Bones were fixed in IHC zinc fixative (BD Pharmingen, San Diego, CA) for 24 h, decalcified in 13% EDTA solution for 2 weeks, and then embedded in paraffin. Longitudinal sections of 5 μ m thickness were stained according to the trichrome method. At a magnification of 1.25 \times (Olympus BX60 Microscope from Olympus, Tokyo, Japan; Zeiss Axio Cam and Axio Vision 3.1 from Carl Zeiss, Oberkochen, Germany; ImageJ Analysis System from NIH, Bethesda, MD) structural indices were calculated according to the suggestions provided by Gerstenfeld et al. [18]. These included total callus

area (bone, cartilaginous, and fibrous callus area)/femoral bone diameter (cortical width plus marrow diameter) at the fracture gap (CAr/BDm [mm]), callus diameter/femoral bone diameter (CDm/BDm), bone (total osseous tissue) callus area/total callus area (TOTAr/CAr [%]), cartilaginous callus area/total callus area (CgAr/CAr [%]), and fibrous tissue callus area/total callus area (FTAr/CAr [%]).

In addition, tartrate-resistant acid phosphatase (TRAP) activity was analyzed in the callus at 2 and 5 weeks after fracture healing ($n = 8$ each group). Therefore, bones were fixed in IHC zinc fixative for 24 h, decalcified in 13% EDTA solution for 2 weeks, and then embedded in paraffin. Longitudinal sections of 5 μm thickness were stained according to the trichrome method. After deparaffinizing again, sections were incubated in a mixture of 5 mg naphotol AS-MX phosphate and 11 mg fast red TR salt in 10 ml 0.2 M sodium acetate buffer (pH 5.0) for 1 h at 37°C. Sections were counterstained with methyl green and covered with glycerin gelatin. TRAP-positive multinucleated cells (three or more nuclei each cell) were counted. In 2-week specimens, one high-power field (HPF, $\times 400$ magnification) was placed in a standardized manner in the central region of the callus (former fracture gap), while five additional HPFs were placed at each site within the periosteal region of the callus. Thus, a total of 11 HPFs were analyzed from each specimen. Because of the reduced size of the callus at 5 weeks, only seven HPFs per specimen were studied (Fig. 1). The data on histomorphological osteoclast analyses are given as numbers of osteoclasts per HPF. In addition, we differentiated between the number of osteoclasts within bone tissue and the number of osteoclasts within cartilaginous tissue.

Western Blot Analysis

The callus tissue was frozen and stored at -80°C until required. Analyses were performed from callus tissue at 2 weeks after fracture healing ($n = 5$ each group). For whole-protein extracts and Western blot analysis of bone morphogenetic protein-2 (BMP-2) and -4 (BMP-4), cysteine-rich protein (CYR) 61, proliferating cell nuclear antigen (PCNA), receptor activator of NF- κB ligand (RANKL), and osteoprotegerin (OPG), the callus tissue was homogenized in lysis buffer (10 mM Tris [pH 7.5], 10 mM NaCl, 0.1 mM EDTA, 0.5% Triton-X 100, 0.02% NaN_3 , 0.2 mM PMSF, and protease inhibitor cocktail [1:100 v/v; Sigma-Aldrich, Taufkirchen, Germany]), incubated for 30 min on ice, and centrifuged for 30 min at $16,000\times g$. Protein concentrations were determined using the Lowry assay. The whole-protein extracts (10 μg protein per lane) were separated discontinuously on sodium dodecyl sulfate polyacrylamide gels and transferred to polyvinylidene difluoride membranes. After blockade of

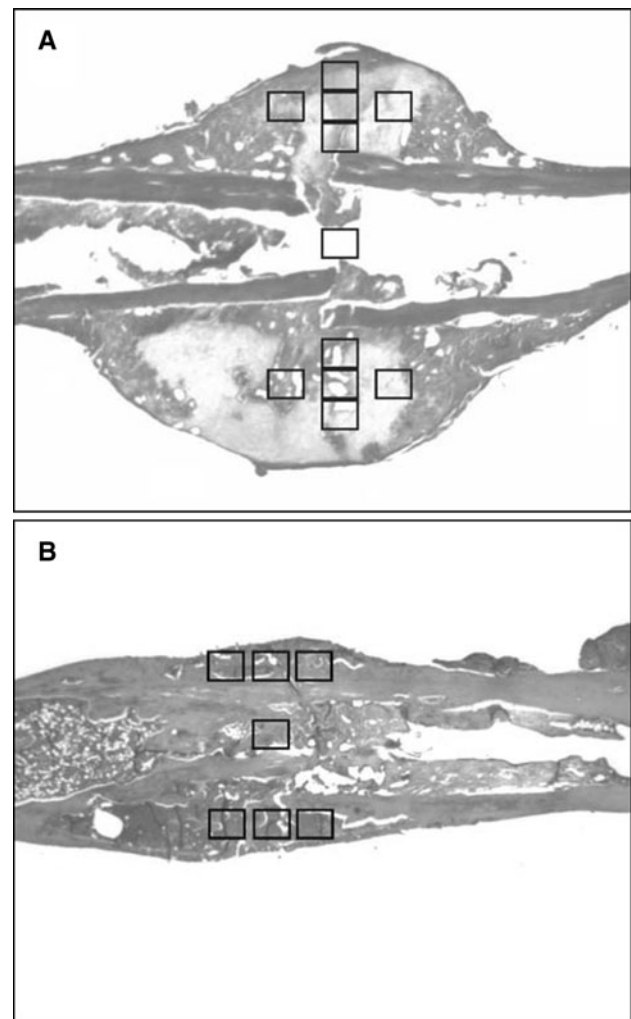


Fig. 1 Schematic representation of the localization of the high-power fields which were studied for analyzing the number of TRAP-positive cells 2 weeks (a) and 5 weeks (b) after fracture

nonspecific binding sites, membranes were incubated for 4 h with the following antibodies: rabbit anti-mouse BMP-2 and rabbit anti-mouse BMP-4 (both 1:100; Santa Cruz Biotechnology, Heidelberg, German), goat anti-mouse CYR61 (1:100, Santa Cruz Biotechnology), mouse anti-mouse PCNA (1:500, Dako Cytomation, Hamburg, Germany), mouse anti-mouse RANKL (Abcam, Cambridge, UK), and rabbit anti-mouse OPG (Santa Cruz Biotechnology). This was followed by corresponding horseradish peroxidase-conjugated secondary antibodies (1.5 h, 1:5,000; GE Healthcare Amersham, Freiburg, Germany). Protein expression was visualized using luminol-enhanced chemiluminescence (GE Healthcare Amersham). Signals were densitometrically assessed (Quantity one, Geldoc, BioRad, Munich, Germany) and normalized to α -tubulin signals (1:20,000, anti- α -tubulin; Sigma-Aldrich) to correct for unequal loading.

Statistical Analysis

All data are given as means \pm SEM. After proving the assumption for normal distribution (Kolmogorov–Smirnov test) and equal variance (*F*-test), the two experimental groups were compared by Student's *t*-test. For nonparametric data, the Mann–Whitney *U*-test was used. Statistics were performed using GraphPad Prism 4.0 software package (Graphpad, San Diego, CA). $p < 0.05$ was considered to indicate a significant difference.

Results

Radiological Analysis

Radiological analyses at 2 and 5 weeks after fracture demonstrated a lower Goldberg score after pantoprazole treatment (0.4 ± 0.2 and 1.7 ± 0.2) compared to controls (0.9 ± 0.3 and 1.8 ± 0.1); however, the differences did not prove to be statistically significant ($p > 0.05$).

Biomechanical Analysis

Biomechanical analysis showed in pantoprazole-treated animals compared to controls a reduced bending stiffness at 2 weeks after fracture (Fig. 2a, c) and a significantly lowered bending stiffness ($p < 0.05$) at 5 weeks after fracture (Fig. 2b, d). This indicates decreased quality of the newly formed bone, in particular at 5 weeks after pantoprazole treatment. The significant difference in bending stiffness between pantoprazole-treated animals and controls was

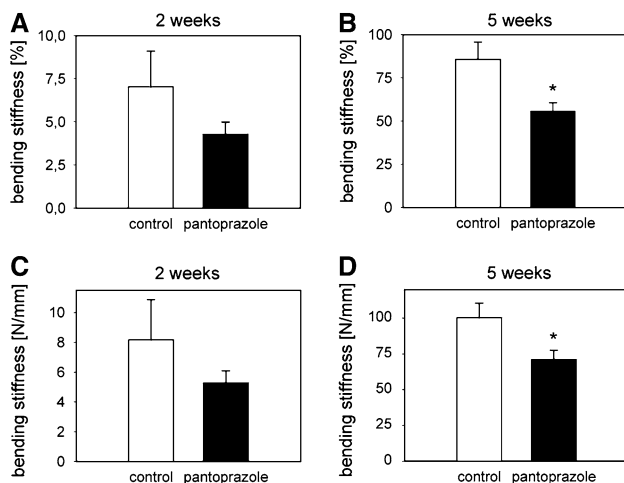


Fig. 2 Biomechanical analysis of bending stiffness at 2 weeks (**a, c**) and 5 weeks (**b, d**) of fracture healing in control (*white bars*) and pantoprazole-treated (*black bars*) animals. Data are given in percent to the contralateral femora (**a, b**) and as absolute values (**c, d**). Means \pm SEM; * $p < 0.05$ vs. control

found when comparing the relative (to nonfractured contralateral bone) bending stiffness data (Fig. 2a, b) but also when comparing the absolute data (Fig. 2c, d). Of interest, comparison of bending stiffness of the nonfractured control femora did not show significant differences between pantoprazole-treated animals and saline-treated animals with 129.8 ± 9.6 vs. $115. \pm 8.6$ N/mm at 2 weeks after fracture and 129.6 ± 8.2 vs. 120.8 ± 9.4 N/mm at 5 weeks after fracture. Therefore, we can conclude that the 5-week pantoprazole treatment did not affect the quality of nonfractured bone.

Histological Analysis

Analysis of the total callus area in relation to the femoral diameter did not show significant differences between the two groups after 2 and 5 weeks of fracture healing (Fig. 3c, d). After 2 weeks the callus of the two groups showed comparable amounts of bone as well as cartilaginous and fibrous tissue (Fig. 3e, g, i). After 5 weeks, however, the amount of bone tissue was significantly lower ($88.6 \pm 5.1\%$ vs. $99.3 \pm 0.3\%$) and the amounts of remnant cartilaginous ($7.8 \pm 4.2\%$ vs. $0.5 \pm 0.2\%$) and fibrous ($3.6 \pm 1.4\%$ vs. $0.2 \pm 0.1\%$) tissue were significantly higher after pantoprazole treatment (Fig. 3a, b, f, h and j).

Analysis of the number of TRAP-positive osteoclasts in the callus at 2 weeks after fracture healing did not show a significant difference between the two groups (Fig. 4). In saline-treated controls almost all positively stained cells were found in the osseous tissue. Only few TRAP-positive osteoclasts were found within the cartilaginous tissue. In pantoprazole-treated animals the amount of positively stained cells within the cartilaginous tissue was higher. However, this difference did not prove to be statistically significant (Fig. 4d). After 5 weeks, only few TRAP-positive osteoclasts could be found in the osseous tissue of the callus of pantoprazole-treated animals, and no positively stained cells were found in the callus of saline-treated controls (Fig. 4c, e).

Western Blot Analysis

After 2 weeks of fracture healing, Western blot analysis of the callus tissue revealed that pantoprazole reduced expression of the bone formation markers BMP-2 ($p < 0.05$), BMP-4 ($p < 0.05$), and CYR61 ($p = 0.056$) (Fig. 5a–d). In addition, expression of PCNA, indicating cell proliferation, was significantly reduced after pantoprazole treatment (Fig. 5e, f). Of interest, expression of OPG, an inhibitor of osteoclastogenesis, was slightly increased in the callus of pantoprazole-treated animals (8.1 ± 1.8 OD * mm^2) compared to controls (6.0 ± 1.0 OD * mm^2), while

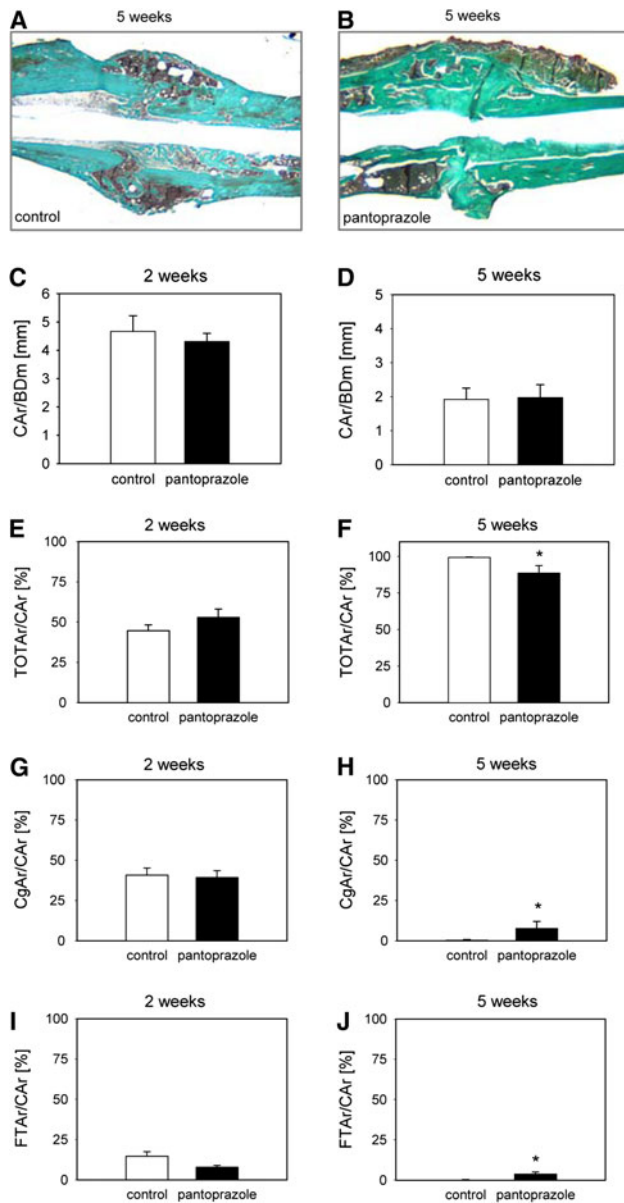


Fig. 3 Representative histological sections after 5 weeks of fracture healing in controls (a) and pantoprazole-treated animals (b). c, d Histomorphometric analysis of the total callus area (CAr) in relation to the diameter of the femur (BDm) after 2 weeks (c) and 5 weeks (d) of fracture healing in control (white bars) and pantoprazole-treated animals (black bars). e–j Histomorphometric analysis of the tissue distribution within the callus area, including total osseous tissue callus area/total callus area (TOTAr/CAr, %) (e, f), cartilaginous tissue callus area/total callus area (CgAr/CAr, %) (g, h), and fibrous tissue callus area/total callus area (FTAr/CAr, %) (i, j) after 2 weeks (e, g, i) and 5 weeks (f, h, j) of fracture healing in controls (white bars) and pantoprazole-treated animals (black bars). Means \pm SEM; * $p < 0.05$ vs. control

expression of RANKL, a stimulator of osteoclastogenesis, was significantly reduced after pantoprazole treatment (Fig. 5e, g). This indicates a significant increase of the OPG/RANKL ratio after pantoprazole treatment.

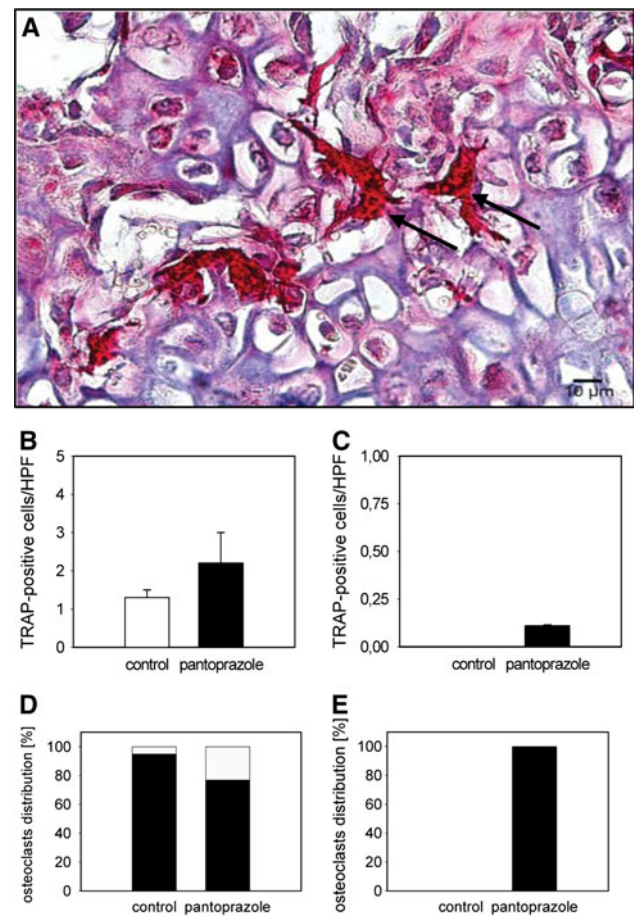


Fig. 4 a Representative histological section of TRAP-positive osteoclasts (arrows) at 2 weeks after fracture healing in pantoprazole-treated animals. b, c Quantitative analysis of the number of TRAP-positive cells per high-power field (HPF) at 2 weeks (b) and 5 weeks (c) in controls (white bars) and pantoprazole-treated animals (black bars). d, e Distribution of osteoclasts (given in percent) within the osseous tissue (black) and cartilaginous tissue (gray) after 2 weeks (d) and 5 weeks (e). Means \pm SEM

Discussion

In the present study, we analyzed the effect of pantoprazole on the process of fracture healing. We demonstrate for the first time that pantoprazole induces a delay of fracture repair, as indicated by a significantly lower bending stiffness and reduced bone formation compared to saline-treated controls. The action of pantoprazole may involve a reduction of osteoclast activity, as indicated by the down-regulation of RANKL. This inhibits bone resorption and delays bone remodeling. However, pantoprazole may also affect cell proliferation and bone formation, as indicated by the significantly reduced expression of PCNA and BMP-4 after pantoprazole treatment.

In general, PPIs are one of the most widely used classes of drugs, but adverse effects receive increasing attention,

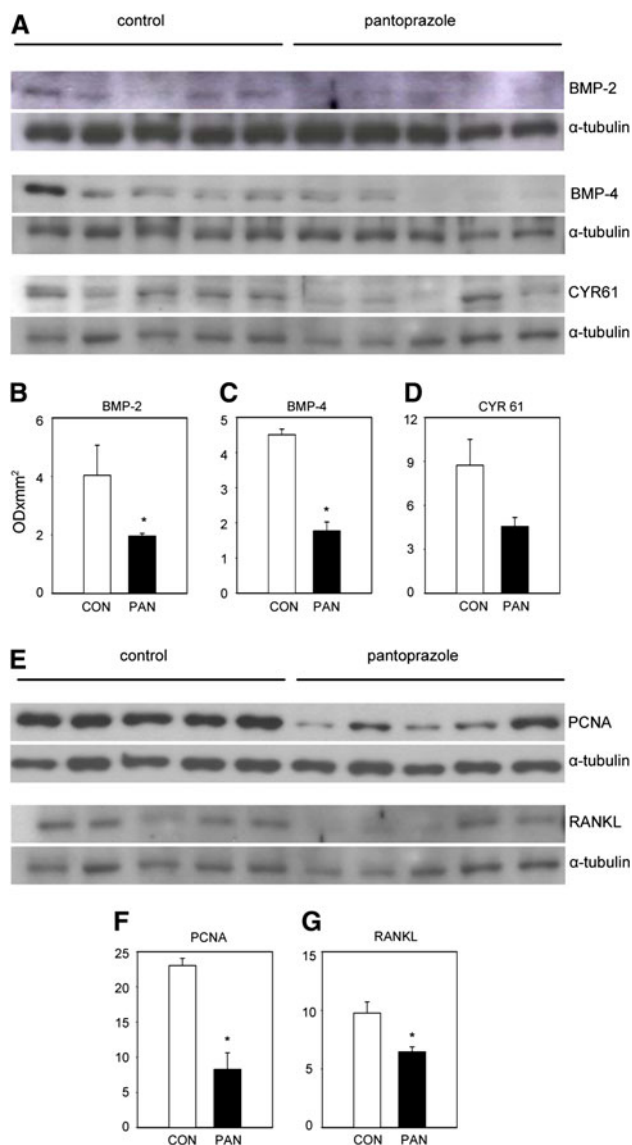


Fig. 5 Western blot analysis of expression of the bone formation markers BMP-2 (a, b), BMP-4 (a, c), and CYR61 (a, d) as well as the proliferation marker PCNA (e, f) and the osteoclastogenesis stimulator RANKL (e, g) in the callus of controls (*white bars*) and pantoprazole-treated animals (*black bars*) after 2 weeks of fracture healing. Means \pm SEM; * $p < 0.05$ vs. control

including an increased incidence of bone fractures [19]. PPIs exert their effect through inhibition of the H^+/K^+ -ATPase enzyme, resulting in a decrease of H^+ secretion, thereby elevating the intragastric pH. Of interest, by investigating specific cellular activities in the bone resorptive process in vitro Zaidi [20] found inhibited osteoclastic bone resorption after treatment with a PPI. A recent study also demonstrated that gastrointestinal PPIs regulate osteoclast-mediated resorption of calcium phosphate cements in vivo [21]. Furthermore, the effect of PPIs on bone resorption has been evaluated in patients who had a history of gastric ulcer. In these patients a lower number of bone resorption markers

was found compared to the control group [11], suggesting that specific inhibitors of the osteoclastic proton pump effectively suppress bone resorption and may thus be useful for the treatment of metabolic bone diseases with increased bone resorption [11]. Visentin et al. [12] analyzed SB 242784, a potent and selective inhibitor of the osteoclastic $V-H^+$ -ATPase, in two animal models of bone resorption. SB 242784 completely prevented retinoid-induced hypercalcaemia in thyroparathyroidectomized rats and bone loss in ovariectomized rats. In line with the results of these studies, the data of the present study demonstrate that the PPI pantoprazole significantly reduces RANKL expression. However, since remodeling during fracture healing requires osteoclast-mediated cartilage and bone resorption, the reduced RANKL expression by pantoprazole may be the cause for a delay in remodeling, as indicated by the significantly lower callus stiffness during the late phase of fracture healing.

Of interest, pantoprazole treatment did not affect the number of TRAP-positive osteoclasts despite the reduction of RANKL expression. However, the inhibition of osteoclast activity, as indicated by the decrease of RANKL expression, may not necessarily be associated with a reduction of the number of osteoclasts. In a previous study, Karsdal et al. [22] demonstrated that the selective proton pump blocker bafilomycin completely inhibits osteoclastic bone resorption and even increases the number of osteoclasts. Also, Hyun et al. [23] showed that the PPI omeprazole significantly increases the OPG/RANKL ratio without affecting TRAP positivity. This is in line with the results of the present study, demonstrating a pantoprazole-induced increase of the OPG/RANKL ratio without affecting the number of TRAP-positive osteoclasts.

In a previous study, Gerstenfeld et al. [24] showed that RANKL inhibition delays the process of remodeling within the fracture callus; however, this was associated with an enhanced stiffness of the healing bone. The reduced stiffness observed in the present study may be due to the fact that pantoprazole affected bone metabolism not only through control of the RANKL/RANK/OPG system but also through a dysregulation of bone formation markers. Furthermore, the callus size of pantoprazole-treated animals was not noteworthy larger than that of controls. This can be a compensatory consequence of the pantoprazole-induced reduction of RANKL expression, achieved by inhibition of bone formation markers.

Apart from reduction of RANKL expression, the present study indicates that pantoprazole also suppresses expression of the bone formation markers BMP-2, BMP-4, and CYR61 during the process of fracture healing. This indicates that pantoprazole affects bone metabolism not only through control of the RANKL/RANK/OPG system but also through the regulation of bone formation. After fracture and

development of a soft callus, this temporary structure is slowly converted into bone by a remodeling process involving the resorption of calcified cartilage and the laying down of new bone [25]. This osteogenic phase is defined by the expression of bone formation markers. The expression of these markers is initiated at 24 h postfracture, although they show a peak in expression between days 14 and 21. During this phase callus becomes mineralized and transforms to hard callus. Thus, a reduction of bone formation markers at days 14–21 may result in reduced callus quality, resulting in a lower bending stiffness at later time points of healing. In fact, the present study shows that pantoprazole treatment delays bone formation and decreases bending stiffness after 5 weeks of fracture healing. This is most probably due to the reduced expression of BMP-2, BMP-4, and CYR61 at 2–3 weeks after fracture.

It is well known that BMPs play an important role in fracture healing [26]. Devlin et al. [27] studied the effects of noggin, a BMP antagonist which binds BMP-4 and blocks BMP signaling. By histological analyses these authors demonstrated in transgenic mice overexpressing noggin decreases of trabecular bone volume, number of trabeculae, and bone formation rate. Furthermore, overexpression of noggin showed decreased expression of some bone formation markers and RANKL, indicating a delay in remodeling after blocking BMPs. This is in line with the results of the present study, demonstrating in parallel reduced expression of BMP-2, BMP-4, and RANKL after pantoprazole treatment.

We focused additionally on the expression of CYR61 because CYR61 is an essential factor for osteoblast functions, including osteogenic commitment of mesenchymal cells, proliferation and maturation of osteoblast precursor cells, and migration of osteoblastic cells. In osteoblastic cells, CYR61 mRNA expression is upregulated by 1,25(OH)vitamin D₃ and the canonical Wnt signaling [28, 29]. Furthermore, CYR61 upregulates BMP-2 mRNA and protein expression, resulting in enhanced cell proliferation and osteoblastic differentiation [30], indicating that CYR61 is an interesting osteogenic marker to analyze bone formation during fracture healing. In the present study pantoprazole markedly decreased the expression of CYR61 and impaired bone healing by reducing the quality of the callus tissue. Decreased CYR61 expression may influence fracture healing by acting in chondrocytes or osteocytes. In a rat fracture model, Hadjiargyrou et al. [31] demonstrated that the highest peak of CYR61 expression correlates with chondrogenesis, indicating that CYR61 plays an important role during endochondral ossification. Besides its action in chondrocytes, CYR61 may also influence fracture healing by acting on osteocytes. Hadjiargyrou et al. [31] could also detect CYR61 in immature osteocytes within newly formed bone and suggested that some growth factors which

regulate fracture repair may also modulate CYR61 expression. This view is further supported by the fact that knock-down of CYR61 significantly diminishes Wnt3A-induced osteogenic differentiation [29]. In addition, CYR61 has been shown to inhibit the formation of bone-resorbing osteoclasts [32] and to stimulate the proliferation and differentiation of bone-forming osteoblasts [33]. Thus, the impaired fracture healing after pantoprazole observed in the present study may be due to a decrease of proliferation and differentiation of bone-forming osteoblasts mediated by the reduced CYR61 expression.

In conclusion, pantoprazole treatment delays fracture repair most probably by affecting both bone formation and bone remodeling through downregulation of bone formation markers and inhibition of osteoclast activity.

Conflict of interest The authors have stated that they have no conflict of interest.

References

1. Ferron GM, McKeand W, Mayer PR (2001) Pharmacodynamic modeling of pantoprazole's irreversible effect on gastric acid secretion in humans and rats. *J Clin Pharmacol* 41:149–156
2. Lindberg P, Nordberg P, Alminger T et al (1986) The mechanism of action of the gastric acid secretion inhibitor omeprazole. *J Med Chem* 29:1327–1329
3. Graziani G, Como G, Badalamenti S et al (1995) Effect of gastric acid secretion on intestinal phosphate and calcium absorption in normal subjects. *Nephrol Dial Transplant* 10:1376–1380
4. O'Connell MB, Madden DM, Murray AM et al (2005) Effects of proton pump inhibitors on calcium carbonate absorption in women: a randomized crossover trial. *Am J Med* 118:778–781
5. Targownik LE, Lix LM, Metge CJ et al (2008) Use of proton pump inhibitors and risk of osteoporosis-related fractures. *CMAJ* 179:319–326
6. Yang YX, Lewis JD, Epstein S, Metz DC (2006) Long-term proton pump inhibitor therapy and risk of hip fracture. *JAMA* 296:2947–2953
7. Yu EW, Blackwell T, Ensrud KE et al (2008) Acid-suppressive medications and risk of bone loss and fracture in older adults. *Calcif Tissue Int* 83:251–259
8. Tucker KL, Hannan MT, Qiao N et al (2005) Low plasma vitamin B₁₂ is associated with lower BMD: the Framingham Osteoporosis Study. *J Bone Miner Res* 20:152–158
9. Farina C, Gagliardi S (2002) Selective inhibition of osteoclast vacuolar H⁺-ATPase. *Curr Pharm Des* 8:2033–2048
10. Tuukkanen J, Väänänen HK (1986) Omeprazole, a specific inhibitor of H⁺-K⁺-ATPase, inhibits bone resorption in vitro. *Calcif Tissue Int* 38:123–125
11. Mizunashi K, Furukawa Y, Katano K, Abe K (1993) Effect of omeprazole, an inhibitor of H⁺,K⁺-ATPase, on bone resorption in humans. *Calcif Tissue Int* 53:21–25
12. Visentin L, Dodds RA, Valente M et al (2000) A selective inhibitor of the osteoclastic V-H⁺-ATPase prevents bone loss in both thyroparathyroidectomized and ovariectomized rats. *J Clin Invest* 106:309–318
13. Bilic I, Zoricic I, Anic T et al (2001) Haloperidol-stomach lesions attenuation by pentadecapeptide BPC 157, omeprazole,

- bromocriptine, but not atropine, lansoprazole, pantoprazole, ranitidine, cimetidine and misoprostol in mice. *Life Sci* 68: 1905–1912
14. Masubuchi N, Hakusui H, Okazaki O (1997) Effects of pantoprazole on xenobiotic metabolizing enzymes in rat liver microsomes: a comparison with other proton pump inhibitors. *Drug Metab Dispos* 25:584–589
 15. Holstein JH, Matthys R, Histing T et al (2008) Development of a stable closed femoral fracture model in mice. *J Surg Res* 153: 71–75
 16. Goldberg VM, Powell A, Shaffer JW et al (1985) Bone grafting: role of histocompatibility in transplantation. *J Orthop Res* 3:389–404
 17. Histing T, Holstein JH, Garcia P et al (2009) Ex vivo analysis of rotational stiffness of different osteosynthesis techniques in mouse femur fracture. *J Orthop Res* 27:1152–1156
 18. Gerstenfeld LC, Wronski TJ, Hollinger JO, Einhorn TA (2005) Application of histomorphometric methods to the study of bone repair. *J Bone Miner Res* 20:1715–1722
 19. Mazziotti G, Canalis E, Giustina A (2010) Drug-induced osteoporosis: mechanisms and clinical implications. *Am J Med* 123: 877–884
 20. Zaidi M (1990) Modularity of osteoclast behaviour and “mode-specific” inhibition of osteoclast function. *Biosci Rep* 10: 547–556
 21. Sheraly AR, Lickorish D, Sarraf F, Davies JE (2009) Use of gastrointestinal proton pump inhibitors to regulate osteoclast-mediated resorption of calcium phosphate cements in vivo. *Curr Drug Deliv* 6:192–198
 22. Karsdal MA, Henriksen K, Sørensen MG et al (2005) Acidification of the osteoclastic resorption compartment provides insight into the coupling of bone formation to bone resorption. *Am J Pathol* 166:467–476
 23. Hyun JJ, Chun HJ, Keum B et al (2010) Effect of omeprazole on the expression of transcription factors in osteoclasts and osteoblasts. *Int J Mol Med* 26:877–883
 24. Gerstenfeld LC, Sacks DJ, Pelis M et al (2009) Comparison of effects of the bisphosphonate alendronate versus the RANKL inhibitor denosumab on murine fracture healing. *J Bone Miner Res* 24:196–208
 25. Marsell R, Einhorn TA (2009) The role of endogenous bone morphogenetic proteins in normal skeletal repair. *Injury* 40:4–7
 26. Tsuji K, Bandyopadhyay A, Harfe BD et al (2006) BMP2 activity, although dispensable for bone formation, is required for the initiation of fracture healing. *Nat Genet* 38:1424–1429
 27. Devlin RD, Du Z, Pereira RC et al (2003) Skeletal overexpression of noggin results in osteopenia and reduced bone formation. *Endocrinology* 144:1972–1978
 28. Schütze N, Lechner A, Groll C et al (1998) The human analog of murine cysteine rich protein 61 is a 1 α ,25-dihydroxyvitamin D₃ responsive immediate early gene in human fetal osteoblasts: regulation by cytokines, growth factors, and serum. *Endocrinology* 139:1761–1770
 29. Si W, Kang Q, Luu HH et al (2006) CCN1/Cyr61 is regulated by the canonical Wnt signal and plays an important role in Wnt3A-induced osteoblast differentiation of mesenchymal stem cells. *Mol Cell Biol* 26:2955–2964
 30. Su JL, Chiou J, Tang CH et al (2010) CYR61 regulates BMP-2-dependent osteoblast differentiation through the $\alpha_v\beta_3$ integrin/integrin-linked kinase/ERK pathway. *J Biol Chem* 285:31325–31336
 31. Hadjiargyrou M, Ahrens W, Rubin CT (2000) Temporal expression of the chondrogenic and angiogenic growth factor CYR61 during fracture repair. *J Bone Miner Res* 15:1014–1023
 32. Crockett JC, Schütze N, Tosh D et al (2007) The matricellular protein CYR61 inhibits osteoclastogenesis by a mechanism independent of $\alpha_v\beta_3$ and $\alpha_v\beta_5$. *Endocrinology* 48:5761–5768
 33. Schütze N, Kunzi-Rapp K, Wagemanns R et al (2005) Expression, purification, and functional testing of recombinant CYR61/CCN1. *Protein Expr Purif* 42:219–225